

Chemical Synthesis of Copper Nanospheres and Nanocubes and Their Antibacterial Activity Against *Escherichia coli* and *Enterococcus sp*

A. Alshareef¹, K. Laird² and R. B. M. Cross^{1*}

¹Emerging Technologies Research Centre, School of Engineering and Sustainable Development, Faculty of Technology, De Montfort University. Leicester, LE1 9BH, United Kingdom; ²Leicester School of Pharmacy, Faculty of Health and Life Sciences, De Montfort University. Leicester, LE1 9BH, United Kingdom.

Abstract: The interest in synthesising inorganic nanomaterials for biological applications has increased in recent years, especially for antibacterial purposes. In the present study, spherical and cube-shaped copper nanoparticles were synthesised by a chemical reduction method and their efficacy as antimicrobial agents against both Gram-negative (*Escherichia coli*) and Gram-positive (*Enterococcus sp*) organisms investigated. The nanoparticles were characterised using ultra-violet/visible spectroscopy, scanning electron microscopy, energy-dispersive spectroscopy and x-ray diffraction. Copper nanocubes were found to be more antimicrobial when compared with copper nanospheres and it is postulated that whilst both sets of nanoparticles have similar total surface areas, the different shapes have different active facets and surface energies, which may lead to differing bactericidal behaviour.

Keywords: Copper nanoparticles, SEM, Antibacterial, *Escherichia coli*, *Enterococcus sp*. PACS: 61.46.+w

*Corresponding author: Dr. R. B. M. Cross (PhD); Tel: +441162506157; email: rcross@dmu.ac.uk

1-INTRODUCTION

The antibacterial properties of nanoparticles depend on a number of factors including the type of microorganism and the physicochemical properties of the nanoparticles [1][2]. The rate of bacterial growth can also affect the tolerance of bacteria to nanoparticles: fast-growing bacteria are more sensitive to nanoparticles than slow-growing bacteria [3]. This is most likely due to the expression of stress-response genes within the bacteria themselves [4]. Copper nanoparticles (CuNPs) have been shown to have a great deal of potential for exploitation in a variety of areas due to their antibacterial properties [5]. These include applications in the textile industry, water disinfection, medicine and food packaging [6], as well as in dentistry to avoid/combat infection [7].

Results from *in vitro* studies in animal models demonstrate size-dependent effects of Cu particles [8]. For example, nano-sized Cu particles have been found to be more toxic than micro-sized Cu particles following oral administration to rats [8]. Cu ions are redox-active, meaning that the high intracellular concentration, which can result after dissolution of CuNPs inside the cell, usually results in great oxidative stress [8]. Signs of oxidative stress and genotoxicity have also been reported after cellular exposure to copper oxide nanoparticles (CuONPs), and include the generation of intercellular reactive oxygen species (ROS) and oxidative DNA lesions [9][10]. However, nanoparticles of Cu and CuO have different mechanisms of toxicity following cell exposure. CuNPs target the cell membrane causing a rapid loss of its integrity, which then leads to cell death. Conversely, CuONPs appear endocytosed within cells in the first hours of interaction which is followed by DNA damage [11].

There are some reports in the literature describing the size-dependent antibacterial activity of nanoparticles of silver (AgNPs) [12]. However, there is very little published work as to how nanoparticle shape might affect the level of antibacterial behaviour. A recent study has suggested that the antibacterial effect of AgNPs may be affected by their total surface area and facet reactivity, whereby AgNPs with larger effective contact areas and more reactive facets exhibit stronger antibacterial activity [13]. In this regard, this paper describes a comparative study of the antibacterial activity of Cu nanospheres (CuNSs) and nanocubes (CuNCs) of the same primary dimension (the diameter of CuNSs/side length of CuNCs were found on average to be approximately 270nm); and the same total surface area per unit mass ($2.480 \text{ m}^2/\text{g}$).

2-EXPERIMENT

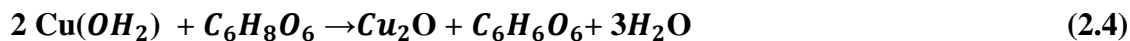
2.1-Materials

All chemicals for this study were purchased from Sigma-Aldrich, UK, without further purification. They include copper sulphate (CuSO_4), ascorbic acid ($\text{C}_6\text{H}_8\text{O}_6$), polyvinylpyrrolidone (PVP) ($[\text{C}_6\text{H}_9\text{NO}]_n$), sodium hydroxide (NaOH) and ethylene glycol (EG) ($\text{C}_2\text{H}_6\text{O}_2$).

2.2-Synthesis of CuNSs

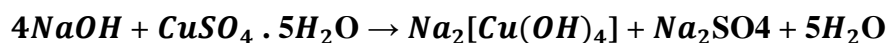
The CuNS growth solution was prepared by adding 1.59g of CuSO_4 , 1g PVP and 4.36g of ascorbic acid to 100ml of de-ionised (DI) water (Milli-Q, $18.2 \text{ M}\Omega\text{cm}^{-1}$). PVP was used as

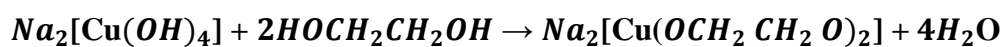
a surfactant and ascorbic acid as a reducing agent. The solution was then stirred and maintained at 80 °C. The formation of CuNPs was confirmed once the colour of the mixture turned brick red from a blue colour. CuSO₄ primarily dissociates to Cu²⁺ and SO₄²⁻ in water, and Cu²⁺ ions are hydrolysed into Cu(OH)₂ as a precursor. Further reduction of Cu(OH)₂ takes place in the presence of ascorbic acid to form Cu₂O. Lastly, Cu₂O is reduced further to form CuNPs. The reaction can be represented as follows [14].



2.3-Synthesis of CuNCs

5g of CuSO₄ and 2.5g NaOH were mixed with 50ml of EG in a three-necked round flask equipped with a condenser and stirred at room temperature before being heated to 160 °C. The colour of the mixture changed from blue to deep blue, to green, to yellow, to yellowish brown and finally to brick red in 1.5 hours. The reaction can be represented as follows [15].





(3.2)



The synthesised nanoparticles of both shapes were centrifuged at 4600rpm three times and washed with DI water to remove any impurities and unreacted precursors; freeze-drying was then used to transform the copper colloid to a powder phase.

2.4-Particle characterisation

The CuNPs were characterised using ultraviolet/visible (UV-VIS) spectroscopy (Evolution 300 UV-VIS, over the wavelength range 300nm to 1000nm), scanning electron microscopy (SEM), energy-dispersive X-ray (EDX) spectroscopy (LEO S430) and X-ray diffraction (XRD) (Bruker D8 Advance diffractometer). The various solutions were drop-cast onto silicon and glass substrates for SEM/EDX and UV-Vis/XRD investigations respectively.

2.5-Antibacterial activity studies

2.5.1-Bacterial strains and culture conditions

To study the antibacterial activity of CuNPs, the Gram-positive bacteria *Enterococcus sp* and Gram-negative bacteria *Escherichia coli* (*E.coli*) were selected as target organisms.

Both bacterial strains were stored in Luria Bertani broth at -80°C and then cultured in nutrient broth (NB) at 37°C for 24 hours.

2.5.2-Screening of CuNPs for antibacterial activity

Antibacterial activity was determined using the disc diffusion method. Initially, 20ml of molten nutrient agar (NA) media was poured into sterilised petri dishes. 100µl of the cultured bacteria was then dispensed and a sterilised spreader was used to spread the bacteria on the surface of the NA. Disc diffusion papers were placed onto the NA followed by the pouring of 50 µl of a 100µg/ml solution of CuNPs onto the disc paper; everything was then incubated for 24 hours and the zone of inhibition was measured from the edge of the disc to the edge of confluent growth.

2.5.3-Determining the growth curve of *E. coli* and *Enterococcus sp* bacteria cells exposed to different concentration of CuNPs

To obtain the growth kinetics curves of bacterial cells exposed to CuNPs, nutrient broth with different concentrations of CuNPs (2500, 1000, 100 and 50µg/ml) were used. 200 µl of the bacteria treated with CuNPs was dispensed into a 96-well plate using a multi-microlitre pipette and then each well was measured for optical density (OD) at 595nm using a spectrophotometer. The results were then compared to a control sample which contained no CuNPs.

3-RESULTS and DISCUSSION

The absorption spectrum of the CuNS solution shown in Figure 1a shows an intense peak at 580nm, which is attributable to the surface plasmon absorption of copper [16]. In Figure 1b CuNCs show three broad peaks observed at 335nm, 450nm and 785nm, respectively. The absorption spectra of metal nanoparticles are mediated by surface plasmon resonances (SPRs) that shift to longer wavelengths as particle size increases. The shape and position of plasmon absorption of CuNPs are mainly dependent on the dielectric medium, particle size and the surface adsorbed species. According to Mie's theory [17], only a single SPR band is expected in the absorption spectra of spherical nanoparticles, while anisotropic particles could increase the number of SPR bands to two or more depending on the particle shape. The number of SPR peaks rises as the symmetry of the nanoparticles decreases. SEM images of prepared CuNSs and CuNCs are shown in Figure 2 (a and b respectively). The spherically-shaped nanoparticles have an average diameter of ~270nm. Figure 2b shows uniformly cube-shaped NPs with sides of length ~270nm. EDX analysis of the CuNPs shows the presence of Cu, silicon (from the substrate) and low levels of oxygen and carbon (Figure 3).

X-ray diffraction data shown in Figure 4 (a and b) confirm the formation of FCC CuNPs. Diffraction peaks at $2\theta = 43.2$ and 74.4 are attributed to (111) and (220) planes of Cu with a cubic phase (JCPDS card no. 04-0836). However, the XRD pattern for CuNSs shows an additional peak indexed as the (220) diffraction of Cu_2O (JCPDS 05-0667) that can be associated with the slow oxidation of metallic CuNPs in air to form CuO.

Disk diffusion data indicate that both shapes inhibit the growth of Gram-positive bacteria and Gram-negative bacteria. Figure 5 illustrates that CuNCs are more active on both bacteria when compared with CuNSs, with zones of inhibition of 17mm and 7mm against *E. coli* and *Enterococcus sp* respectively. This compares to inhibition zones of 12mm against *E. coli* and 5mm against *Enterococcus sp* for CuNSs (Figure 6).

Figure 7 (a and b) shows the growth kinetics of *E. coli* and *Enterococcus sp* treated with CuNSs. The growth of *E.coli* treated with 2500, 1000, 100 and 50µg of CuNSs was inhibited after 4 hours, while the growth of *Enterococcus sp* was inhibited after 2 hours apart from the highest concentration - the results of which may have been affected by nanoparticle-enhanced scattering. Figure 8 (a and b) shows the growth curves of bacteria treated with all concentrations of CuNCs. Inhibition was again evident after 2-4 hours for *E.coli* and for *Enterococcus sp* after 2h for the lower concentrations only, with the highest seemingly taking longer to take effect (most likely due to enhanced scattering once more).

The better inhibitory effects that were observed in *E. coli* compared to *Enterococcus sp* for both shapes are related to the difference in the outer casing of these bacteria. A Gram-positive bacterium, such as *Enterococcus sp*, has a thick layer of peptidoglycan. In contrast, a Gram-negative bacterium, such as *E. coli*, has an outer membrane covering a thin layer of peptidoglycan. The positive Cu ions released from the NPs may be attracted to the negatively charged bacterial cell walls which may then be ruptured or compromised by the NPs in question; this can lead to protein denaturation followed by cell death [18]. For Gram-negative bacteria with a thinner outer casing, this is likely to occur more readily

which would help to explain the difference in the levels of inhibition here. Moreover, there is also the possibility that the active facets of differently-shaped nanoparticles could be affecting directly their antibacterial behaviour.

It has been argued previously that the reactivity of silver is greater when high atomic density facets are present such as the (111) plane [19]. In this regard, the XRD data for CuNCs in this work shows a higher intensity of (111) when compared with CuNSs. This could be expected as quasi-spherical particles tend to exhibit lower levels of (111) facets [20]. Hence it is postulated that it is the higher reactivity of the CuNCs here that leads to increased antibacterial activity. The higher reactivity may result in the Cu^+ ion binding more readily causing damage to cellular functions by, for example, disrupting the osmotic pressure equilibrium and causing local pH changes. Work is ongoing to ascertain more fully the mechanisms involved and the potential for nanoparticle ingress within the cells themselves.

4-CONCLUSION

In this study, CuNSs and CuNCs were synthesised by a chemical reduction method in water and EG respectively. The particles were characterised by SEM, EDX, XRD and UV-VIS spectroscopy. Studies of the antibacterial activity of the different CuNPs show that whilst both shapes were effective in inhibiting the growth of Gram-positive bacteria and Gram-negative bacteria, CuNCs had the greatest effect. This suggests that whilst the CuNPs have similar surface areas, it is the different shapes and in particular the differing levels of

surface reactivity that contribute to the demonstrated behaviour. The highly-reactive (111) facet was more prevalent in the CuNCs compared with CuNSs and this higher reactivity may be the principal cause that ultimately led to cell death more rapidly in both bacterial strains studied.

REFERENCES

1. W. Witte, *Infect. Genet. Evol.*, **4** (3), 187 . (2004)
2. M. R. Brown, D.G. Allison, P. Gilbert, *J. Antimicrob. Chemother.*, **22** (6), 777 (1988).
3. C. Lu, M. J. Brauer and D. Botstein, *Mol. Biol. Cell*, **20** (3), 891 (2009).
4. G. Ren, D. Hu, E. W. Cheng, M. A. Vargas-Reus, P. Reip, R. P. Allaker, *Int. J. Antimicrob. Agents*, **33** (6), 587 (2009).
5. A. Jamshidi, M. Jahangiri, *Asian J. of Bio. Sci.* **7** (4): 183 (2014)
6. R. P. Allaker, *J. Dent. Res.*, **89** (11), 1175 (2010).
7. I. Subhankari, P. L. Nayak, *World J. of Nano Sci. & Tech.* **2** (1): 10 (2013).
8. Z. Chen, H. Meng, G. Xing, C. Chen, Y. Zhao, G. Jia, T. Wang, H. Yuan, C. Ye, F. Zhao, Z. Chai, C. Zhu, X. Fang, B. Ma, L. Wan, *Toxicol. Lett.*, **163** (2), 109 (2006).
9. M. Ahamed, M. A. Siddiqui, M. J. Akhtar, I. Ahmad, A. B. Pant, H. A. Alhadlaq, *Biochem. Biophys. Res. Commun.*, **396** (2), 578 (2010).
10. N. Hanagata, F. Zhuang, S. Connolly, J. Li, N. Ogawa, M. Xu, *ASC Nano*, **5** (12), 9326 (2011).
11. K. Midander, P. Cronholm, H. L. Karlsson, K. Elihn, L. Möller, C. Leygraf, I. Odnevall-Wallinder, *Small*, **5** (3), 389 (2009).

12. Z. Lu, K. Rong, J. Li, H. Yang, R. Chen, *J. of Mat. Sci.: Materials in Medicine*, **24** (6) 1465 (2013).
13. X. Hong, J. Wen, X. Xiong, Y. Hu, *Envir. Sci. and Poll. Res.*, **5** (23), 4489 (2016).
14. P. Gurav, S. Naik, K. Ansari, S. Srinath, K. Kishore, *Coll. and Surf. A*, **441** 589 (2014).
15. J. Sun, Y. Jing, Y. Jia, M. Tillard, C. Belin, *Mat. Lett.* **59** (29), 3933 (2005).
16. S. Pal, Y. K. Tak, J. M. Song, *Appl. Environ. Microbiol.* **73** (6) 1712 (2007)
17. G. Mie, *Ann. Phys*, **25** (3), 377. (1976).
18. T. Theivasanthi, M. Alagar, arXiv preprint arXiv:1110.1372.
19. D. W.Hatchett, S. Henry, *J. Phys. Chem.* **100** 9854 (1996).
20. B. Wiley, B., Y. Sun, B. Mayers, Y. Xia, *Chem. Eur. J.* **11** 454 (2005).

List of figures

Figure 1: UV-VIS spectra of CuNPs (a) CuNSs and (b) CuNCs.

Figure 2: SEM micrograph of (a) CuNSs and (b) CuNCs ; (scale bar - 300nm)

Figure 3: EDX of (a) CuNSs and (b) CuNCs.

Figure 4: XRD pattern confirming the formation of CuNPs: (a) CuNSs and (b) CuNCs.

Figure 5: The disc diffusion method shows inhibition zones against *Enterococcus* sp for (top left) CuNSs and (top right) CuNCs, and inhibition zones against *E. coli* for (bottom left) CuNSs and (bottom right) CuNCs

Figure 6: Annular radii of zones of inhibition of CuNCs and CuNSs against *E.coli* and *Enterococcus* sp.

Figure 7: (a) Growth curves of E.coli treated with different concentrations (ug/ml) of CuNSs ; (b) Growth curves of Enterococcus sp treated with different concentrations of CuNSs.

Figure 8: (a) Growth curves of E.coli treated with different concentrations of (ug/ml) of CuNCs ; (b) Growth curves of Enterococcus sp treated with different concentrations of CuNCs.